AD-A079 715 STANFORD UNIV CA EDWARD L GINZTON LAB F/G 20/3
ELASTIC DOMAIN WALL WAVES IN FERROELECTRIC CERAMICS AND SINGLE --ETC(U)
JAN 80 B A AULD N00014-79-C-0222
UNCLASSIFIED GL-3076 NL

| OF |
AD-
A079715

END
DATE
FILMED
2-80
DDC

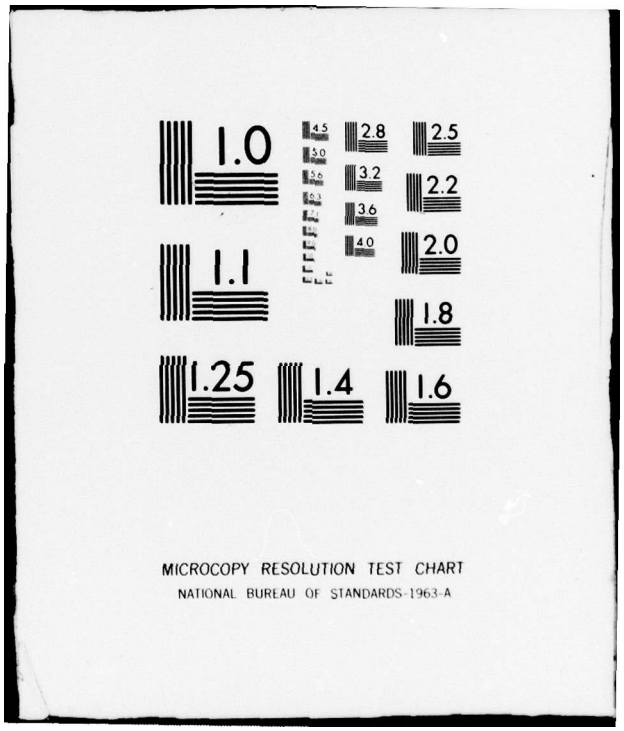
1.0
1.1
1.25
1.4
1.6
1.8
2.0
2.2
2.5
2.8
3.2
3.6
4.0
4.5
5.0
5.6
6.3
MICROCOPY RESOLUTION TEST CHART
NATIONAL BUREAU OF STANDARDS-1963-A

LEVEL II

# (6) ELASTIC DOMAIN WALL WAVES IN FERROELECTRIC CERAMICS AND SINGLE CRYSTALS.

(12)

AD A079715

(9) Annual Progress Report.

1 Feb 79 — 31 Jan 80,

Contract No. N00014-79-C-0222

(15)

(14) GL-

G.L. Report No. 3076

(11) Jan 80

(12) 30

Principal Investigator

(10) B. A. Auld

DDC FILE COPY

Reproduction in whole or in part is permitted by the United States Government

Edward L. Ginzton Laboratory
W. W. Hansen Laboratories of Physics
Stanford University, CA.
Stanford, California

DDC RECEIVED JAN 22 1980 D

DISTRIBUTION STATEMENT A
Approved for public release;
Distribution Unlimited

409 640 80 1 21 089

UNCLASSIFIED

SECURITY CLASSIFICATION OF THIS PAGE (When Data Entered)

| REPORT DOCUMENTATION PAGE | | READ INSTRUCTIONS BEFORE COMPLETING FORM |
|---|---|---|
| 1. REPORT NUMBER | 2. GOVT ACCESSION NO. | 3. RECIPIENT'S CATALOG NUMBER |
| 4. TITLE (and Subtitle)<br>ELASTIC DOMAIN WALL WAVES IN FERROELECTRIC CERAMICS AND SINGLE CRYSTALS | | 5. TYPE OF REPORT & PERIOD COVERED<br>Annual Progress Report<br>1 Feb. 1979 – 31 Jan. 1980 |
| | | 6. PERFORMING ORG. REPORT NUMBER<br>G.L. Report No. 3076 |
| 7. AUTHOR(s)<br>B. A. Auld | | 8. CONTRACT OR GRANT NUMBER(s)<br>N00014-79-C-0222 |
| 9. PERFORMING ORGANIZATION NAME AND ADDRESS<br>Edward L. Ginzton Laboratory<br>W.W. Hansen Laboratories of Physics<br>Stanford University, Stanford, CA 94305 | | 10. PROGRAM ELEMENT, PROJECT, TASK AREA & WORK UNIT NUMBERS |
| 11. CONTROLLING OFFICE NAME AND ADDRESS<br>Director, Metallurgy & Ceramics Program<br>Office of Naval Research<br>800 N. Quincy St., Arlington, VA 22217 | | 12. REPORT DATE<br>January 1980<br>13. NUMBER OF PAGES<br>29 |
| 14. MONITORING AGENCY NAME & ADDRESS(if different from Controlling Office) | | 15. SECURITY CLASS. (of this report)<br>UNCLASSIFIED<br>15a. DECLASSIFICATION/DOWNGRADING SCHEDULE |

16. DISTRIBUTION STATEMENT (of this Report)

Approved for Public Release -- Distribution Unlimited

17. DISTRIBUTION STATEMENT (of the abstract entered in Block 20, if different from Report)

18. SUPPLEMENTARY NOTES

19. KEY WORDS (Continue on reverse side if necessary and identify by block number)

Piezoelectricity
Electrostriction,
Domain Walls,
Ferroelectric Ceramics,
Guided Waves,
Elastic Waveguides,
Elastic Wave Scattering,
Induced Piezoelectricity,
Layered Ceramics Wave Trapping,
Numerical Methods

20. ABSTRACT (Continue on reverse side if necessary and identify by block number)

A theoretical formulation is given for solving problems of elastic waveguiding by and wave scattering at a "duct" consisting of a spatial variation of material parameters with an arbitrary profile function. Both nonpiezoelectric and piezoelectric materials are treated. For the latter case, examples of calculated displacement and electric potential fields are given for several guided modes and several widths of duct.

DD FORM 1 JAN 73 1473 EDITION OF 1 NOV 65 IS OBSOLETE

UNCLASSIFIED

SECURITY CLASSIFICATION OF THIS PAGE (When Data Entered)

# 1. Introduction

The aim of the research is to investigate use of new types of elastic waves as probes for examining the material properties of piezoelectric and electrostrictive types of ferroelectric ceramics and single crystals. This is for the purpose of shedding light on the effectiveness and general characteristics of fabrication techniques, as well as exploring basic physical mechanisms playing a role in the technology of this class of materials. In the category of relevant physical mechanisms, one can cite poling phenomena and grain boundary effects. This study is regarded generally as influencing improvements in and quality control of existing materials, as well as the evaluation of new materials. A possible spin-off could be the invention of switchable domain wall elastic waveguides for electronic signal processing.

During the present report period our effort has been directed toward developing new methods for analyzing wave guidance or scattering from a domain wall of arbitrary profile in a material with general elastic anisotropy and piezoelectricity. The wave guidance (or ducting) of acoustic waves in gases and liquids has already been extensively analyzed, using principally the WKB approximation. This analytical approach, which is also widely used in the analysis of quantum mechanical energy levels for an arbitrary potential function, requires that the mechanical properties be essentially constant over distances comparable to the characteristic wavelength of the medium. For a domain wall structure, this is not an acceptable limitation, even in the purely elastic case. Furthermore, the WKB approach turns out to be extremely unwieldy when the piezoelectric effect is added.

We have developed, for general symmetric domain structure — the normal case — a simple numerical trial integration method that treats structures of arbitrary sharpness and anisotropy. This technique, which has been found to converge rapidly and inexpensively, has been applied to both the isotropic elastic problem and to the simplest known case of a piezoelectric domain wall. In the first example the numerical results agree with WKB when the latter technique is applicable, and in the second example the results agree with published results for wave propagation along a zero-thickness piezoelectric domain wall of the same type. The same general numerical trial integration technique has also been found to be applicable to the calculation of wave scattering from an arbitrary domain wall of symmetric profile, although no examples have yet been treated.


Accession For
NTIS GRA&I
DDC TAB
Unannounced
Justification
By
Distribution/
Availability Codes
Dist. | Avail and/or special
A

DDC
RECEIVED
JAN 22 1980
D

## 2. Domain Wall Waveguiding

### 2.1 Formulation of the Waveguiding Problem for a "Duct" in an Isotropic Medium

This year we developed a theory to handle some specific cases of domain wall waveguiding. In all cases, we restricted our inquiries to shear wave propagation in the x-y plane, with polarization along the z-axis and axes chosen such that the domain wall region was centered in the y-z plane (Fig. 1). The regions were assumed to be infinite in all directions, and the fields were taken to be uniform in the z-direction.

The first case we treated was waveguiding in a nonhomogeneous isotropic elastic medium, where stiffness $c_{IJ}(x)$ and density $\rho(x)$ are functions providing a "slow velocity" region (or duct) capable of guiding a shear wave along the plane $x = 0$. This problem was intended to be only an overture to the more pertinent problem of the piezoelectric domain wall. Our intent in the isotropic case was to model a domain wall as a region of lower stiffness, and hence, assuming a constant density, as a region where waves propagate with a slower shear velocity exists. By solving the acoustic field equations, we hoped to gain some familiarity with the type of modes which could exist in these relatively simple isotropic "domain walls".

By writing the velocity vector as:

$$\underline{v} = \begin{bmatrix} 0 \\ 0 \\ v \end{bmatrix} \quad \text{where} \quad v = v(x,y)$$

and assuming that all fields have a $e^{i\omega t}$ time-dependence, we can compute the

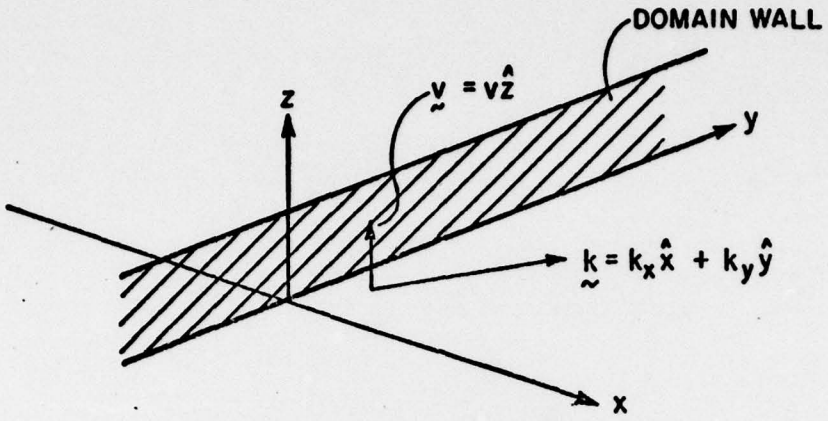


FIG. 1--Basic geometry for the study of shear-type domain wall waves in an infinite medium uniform in $z$ .

relevant components of the acoustic strain field $S_J$ (where $J = 1,2,\ldots,6$) from the equation[1]

$$S_J = \frac{1}{i\omega} \nabla_{Jk} v_k \quad , \quad k = 1,2,3 \tag{1}$$

For the case assumed in Fig. 1 we have $S_1 = S_2 = S_3 = S_6 = 0$ and

$$S_4 = \frac{1}{i\omega} \frac{\partial v}{\partial y} \qquad S_5 = \frac{1}{i\omega} \frac{\partial v}{\partial x} \tag{2}$$

where we have used the fact that $\partial v/\partial z = 0$. The stress $T_I$ ($I = 1,2,\ldots,6$) can now be written using the constitutive relation

$$T_I = c_{IJ} S_J \tag{3}$$

where $c_{IJ}$ is the $6 \times 6$ stiffness matrix and each component is a function of $x$. Using our expressions for $S_J$ in this equation yields $T_1 = T_2 = T_3 = T_6 = 0$ and

$$T_4 = c_{44} \frac{1}{i\omega} \frac{\partial v}{\partial y} \quad ; \quad T_5 = c_{44} \frac{1}{i\omega} \frac{\partial v}{\partial x} \tag{4}$$

Finally, we use the equation of motion

$$\nabla_{kI} T_I = i\omega\rho v_k \quad , \tag{5}$$

which yields two trivial equations ($0 = 0$) and

$$\frac{\partial T_4}{\partial y} + \frac{\partial T_5}{\partial x} = i\omega\rho v \tag{6}$$

Substituting Eq. (4) into Eq. (6) yields

$$c_{44}(x)\,\frac{\partial^2 v(x,y)}{\partial y^2} + \frac{\partial}{\partial x}\left(c_{44}(x)\,\frac{\partial v(x,y)}{\partial x}\right) = -\omega^2 \rho(x)\, v(x,y) \qquad (7)$$

Now, assuming that the wave propagates with an $e^{-i\beta y}$ variation along the y-axis in Fig. 1,

$$v(x,y) = V(x)\, e^{-i\beta y} \qquad (8)$$

our equation becomes an ordinary differential equation of the Sturm-Liouville type,

$$\frac{d}{dx}\left(c_{44}(x)\,\frac{dV(x)}{dx}\right) + \left[\omega^2 \rho(x) - \beta^2 c_{44}(x)\right] V(x) = 0 \quad . \qquad (9)$$

Equation (9) can be transformed into a simple Schrödinger equation by making the substitution

$$\psi(x) \equiv \sqrt{c_{44}(x)}\, V(x)$$

$$g(x) \equiv \omega^2 \frac{\rho(x)}{c_{44}(x)} + \frac{1}{4}\left[\frac{c'_{44}(x)}{c_{44}(x)}\right]^2 - \frac{1}{2}\left[\frac{c''_{44}(x)}{c_{44}(x)}\right] \quad , \qquad (10)$$

and now becomes

$$\frac{d^2\psi}{dx^2} + [g(x) - \beta^2]\psi = 0 \qquad (11)$$

which can be solved numerically, or under the right conditions, analytically, using the WKB approximation. We will not report the results for this case in

detail, since most of the isotropic results are subsumed in the piezoelectric case which follows. Suffice it to say that Eq. (11) is a completely general result independent of the form of $c_{44}(x)$ or $\rho(x)$. Waveguiding phenomena can be studied by assuming appropriate functional forms for $c_{44}(x)$ and $\rho(x)$, so as to provide a "duct" at the plane $x = 0$.

As a general qualitative rule, we can see from Eq. (11) that waves are propagating in regions where $g(x) - \beta^2 > 0$ and evanescent in regions where $g(x) - \beta^2 < 0$. This follows from Eq. (11), and the fact that $\psi''(x) + K^2\psi(x) = 0$ has solutions of the form $\psi(x) = A \sin Kx + B \cos Kx$, and $\psi''(x) - K^2\psi(x) = 0$ has solutions of the form $\psi(x) = ce^{-Kx} + De^{Kx}$. In our work on wave guidance (or "ducting"), we want to have a function $g(x)$ with a local maximum at the origin (corresponding to a shear velocity with a local minimum at the origin). We see that there will be a maximum and a minimum allowed value of $\beta^2$ if we are to have a trapping of energy (or waveguiding) in the vicinity of $x = 0$.

For waveguiding to occur, the solution to Eq. (11) must become exponential as $|x| \to \infty$. This means that $g(x) - \beta^2 < 0$ for large $|x|$ and that $g(x) - \beta^2 = 0$ at some set of points $x = \pm d$ (Fig. 2(a)). These are the turning points between trapping and evanescent regions. Assuming that Eq. (11) has turning points, we can see graphically that solutions with larger $\beta^2$ are damped at a more rapid rate as $x$ increases, and have turning points which are closer to the origin. Therefore, these solutions are trapped more effectively than modes having smaller $\beta^2$. Since $\omega$ is fixed for all, it is clear that the slower waves, with larger $\beta$ — and therefore, smaller $V = \omega/\beta$, are the ones which are the most effectively trapped.

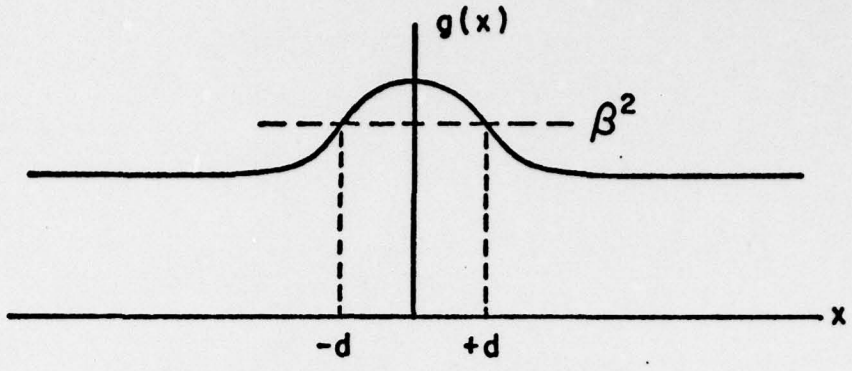


(a)

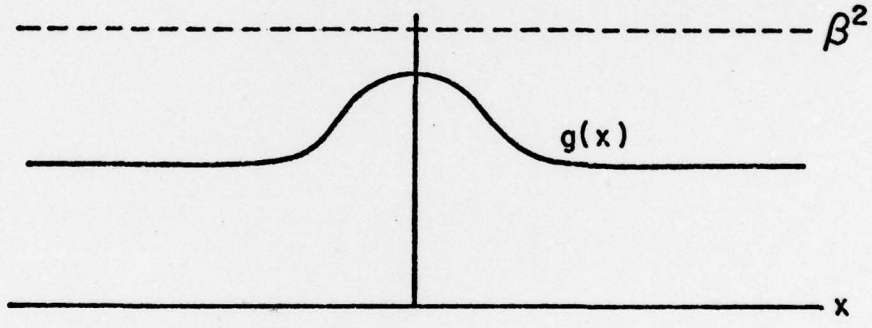


(b)

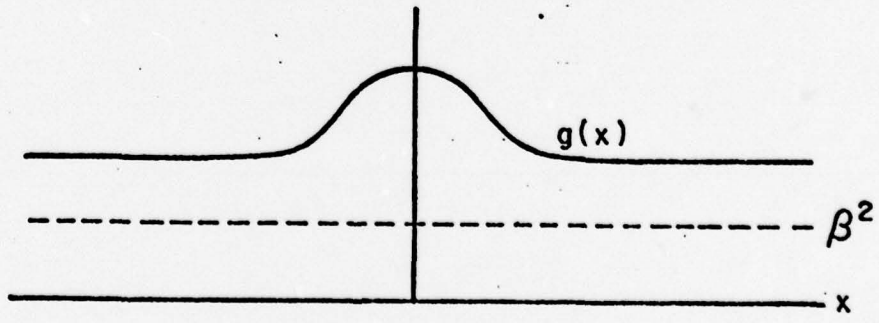


(c)

FIG. 2--(a) Wave is <u>trapped</u> in region $|x| \leqslant d$ and evanescent elsewhere.
(b) Wave cannot propagate, $g(x) - \beta^2 < 0$ for all $x$.
(c) Wave radiates laterally (i.e., no trapping), $g(x) - \beta^2 > 0$ for all $x$.

## 2.2 Waveguiding at a Piezoelectric Domain Wall

After this semiquantitative preface to waveguiding, we now include piezoelectricity to the theory. This inclusion is necessary, since ferroelectric domain walls necessarily involve the piezoelectric effect. Once again, we assume that the domain wall lies in the y-z plane (Fig. 1) and that the acoustic waves are shear waves polarized in the z-direction. We now study, as the simplest example, a hexagonal 6 mm piezoelectric ceramic, such as PZT, with its poling direction taken to be the z-axis. The constitutive relations can be written:

$$
\begin{aligned}
T_1 &= c_{11}^E S_1 + c_{12}^E S_2 + c_{13}^E S_3 - e_{31} E_3 \\
T_2 &= c_{12}^E S_1 + c_{11}^E S_2 + c_{13}^E S_3 - e_{31} E_3 \\
T_3 &= c_{13}^E S_1 + c_{13}^E S_2 + c_{33}^E S_3 - e_{33} E_3 \\
T_4 &= c_{44}^E S_4 - e_{15} E_2 \\
T_5 &= c_{44}^E S_5 - e_{15} E_1 \\
T_6 &= c_{66}^E S_6
\end{aligned}
\tag{12}
$$

and

$$
\begin{aligned}
D_1 &= e_{15} S_5 + \varepsilon_{11}^S E_1 \\
D_2 &= e_{15} S_4 + \varepsilon_{11}^S E_2 \\
D_3 &= e_{31} S_1 + e_{31} S_2 + e_{33} S_3 + \varepsilon_{33}^S E_3
\end{aligned}
\tag{13}
$$

where $\underline{D}$ is electric displacement and $\underline{E}$ is electric field. We now wish

to express strain, $\underset{\sim}{S}$ and electric field, $\underset{\sim}{E}$, in terms of particle displacement $\underset{\sim}{u}$ and electric potential $\phi$. Assuming that the fields are uniform in $z$, we write

$$\underset{\sim}{u} = \begin{bmatrix} 0 \\ 0 \\ u \end{bmatrix} \quad \text{where} \quad u = u(x,y)$$

and

$$\phi = \phi(x,y)$$

Hence $S_1 = S_3 = S_2 = S_6 = 0$ and

$$S_5 = \frac{\partial u}{\partial x} \quad ; \quad S_4 = \frac{\partial u}{\partial y} \tag{14}$$

$$E_1 = -\frac{\partial \phi}{\partial x} \quad ; \quad E_2 = -\frac{\partial \phi}{\partial y} \quad ; \quad E_3 = 0 \tag{15}$$

Therefore, we have $T_1 = T_2 = T_3 = T_6 = 0$, and our only nontrivial equation of motion is

$$\frac{\partial T_5}{\partial x} + \frac{\partial T_4}{\partial y} = \rho \frac{\partial^2 u}{\partial t^2} \; . \tag{16}$$

Also, the condition $\nabla \cdot \underset{\sim}{D} = 0$ must be satisfied throughout the region, so that

$$\frac{\partial D_1}{\partial x} + \frac{\partial D_2}{\partial y} = 0 \tag{17}$$

Substituting Eqs. (14) and (15) into the constitutive relations (12) and (13), and substituting these results into the equations of motion (16) and (17),

we get

$$\rho \frac{\partial^2 u}{\partial t^2} = \frac{\partial}{\partial x}\left[c_{44}^E \frac{\partial u}{\partial x} + e_{15} \frac{\partial \phi}{\partial x}\right] + \frac{\partial}{\partial y}\left[c_{44}^E \frac{\partial u}{\partial y} + e_{15} \frac{\partial \phi}{\partial y}\right]$$

$$0 = \frac{\partial}{\partial x}\left[e_{15} \frac{\partial u}{\partial x} - \varepsilon_{11}^S \frac{\partial \phi}{\partial x}\right] + \frac{\partial}{\partial y}\left[e_{15} \frac{\partial u}{\partial y} - \varepsilon_{11}^S \frac{\partial \phi}{\partial y}\right] \qquad (18)$$

Equations (18) are simplified by taking out the y and t dependence

$$u(x,y,t) = U(x)\, e^{i(\beta y - \omega t)}$$

$$\phi(x,y,t) = \Phi(x)\, e^{i(\beta y - \omega t)}$$

We also recall that $\rho$, $c_{44}^E$, $e_{15}$, $\varepsilon_{11}^S$ are all arbitrary functions of x. For simplicity in what is to follow, we will define:

$$c_{44}^E(x) \equiv c(x) \quad , \quad e_{15}(x) \equiv e(x) \quad , \quad \varepsilon_{11}^S(x) \equiv \varepsilon(x)$$

The equations then become two coupled ordinary differential equations

$$\frac{d}{dx}\left[c \frac{dU}{dx}\right] + (\rho\omega^2 - c\beta^2)U = -\frac{d}{dx}\left[e \frac{d\Phi}{dx}\right] + e\beta^2\Phi$$

$$\frac{d}{dx}\left[e \frac{dU}{dx}\right] - e\beta^2 U = \frac{d}{dx}\left[\varepsilon \frac{d\Phi}{dx}\right] - \varepsilon\beta^2\Phi \qquad (19)$$

In our work, we wish to solve these equations numerically. By making the following substitutions:

$$\frac{dU}{dx} = W$$

$$\frac{d\Phi}{dx} = \Theta$$

we obtain four coupled first order equations,

$$
\begin{aligned}
U' &= W \\
\Phi' &= \Theta \\
W' &= \beta^2 U - \frac{1}{c\varepsilon + e^2}\left\{\varepsilon\rho\omega^2 U + (ee' + \varepsilon c')\, W + (\varepsilon e' - e\varepsilon')\Theta\right\} \\
\Theta' &= \beta^2 \Phi - \frac{1}{c\varepsilon + e^2}\left\{e\rho\omega^2 U + (ee' + c\varepsilon')\,\Theta + (ec' - ce')\, W\right\} ,
\end{aligned}
\tag{20}
$$

where the primes denote differentiation with respect to $x$ .

## 2.3 Numerical Method of Solution

We want a general technique for solving Eqs. (20). The technique must consist of choosing an appropriate $\beta^2$ (the eigenvalue) such that a trapped mode does exist, and then determining the functions $U$ and $\Phi$ from numerical integration of Eqs. (20). In our piezoelectric domain wall problem, the only change in the ceramic from one side to the other of the domain transition region is a gradual reversal in polarization $P$ . If we can describe this polarization profile by an antisymmetric function $P(x)$ , then we can conclude from the transformation properties of the permittivity, piezoelectric, and stiffness matrices that $\varepsilon(x)$ and $c(x)$ are even functions and $e(x)$ is an odd function of $x$ . We also insist that the solution functions $U(x)$ and $\Phi(x)$ be smooth and continuous throughout the region (for a smooth and continuous polarization profile $P(x)$). Moreover, from

the symmetries and antisymmetries of our problem, we conclude that $U(x)$ and $\Phi(x)$ should reflect these symmetries and antisymmetries. Therefore, we look for solutions that are either even or odd in $x$.

If $U(x)$ is even (so that $W(x) = U'(x)$ is odd) we see from Eqs. (20) that $\Phi(x)$ must be odd. Similarly, if $U(x)$ is odd, we see from the equations that $\Phi(x)$ will be even. This information will play an important part in determining $\beta^2$. Going back to Eq. (20) we note that solutions for the $U(x)$ even mode will have the properties:

$$U'(0) = W(0) = 0$$
$$\Phi(0) = 0 \tag{21}$$

at $x = 0$ and solutions for the $U(x)$ odd mode will have:

$$\Phi'(0) = \Theta(0) = 0$$
$$U(0) = 0 \tag{22}$$

at $x = 0$. Our numerical integration technique consists of picking trial values for $U(x)$, $W(x)$, $\Phi(x)$, $\Theta(x)$ at a point $z = a > 0$ that is sufficiently outside the domain wall, in a region where analytical solutions can be derived. The meaning of the term "sufficiently outside" is that the starting point should lie in the flat part of the profile curves in Fig. 2. With these "initial values", we pick a value for $\beta^2$, and numerically integrate our equations in to $x = 0$. Note that the initial values, as well as the actual equations of motion, depend on the choice of $\beta^2$. We continue to pick $\beta^2$, each time integrating to $x = 0$, until either

Eq. (21) or Eq. (22) is satisfied (depending on which mode symmetry we are seeking).

As noted above, the analytic solutions at large $x$ occur in regions where $c(x)$, $\varepsilon(x)$, $e(x)$ are essentially constant, so that $c'(x) = \varepsilon'(x) = e'(x) = 0$. In this region, Eq. (20) becomes

$$U''(x) = \left[\beta^2 - \frac{\varepsilon\rho\omega^2}{c\varepsilon + e^2}\right] U(x) \qquad \text{(a)}$$

$$\Phi''(x) = \beta^2\Phi(x) - \frac{e\rho\omega^2}{c\varepsilon + e^2} U(x) \qquad \text{(b)} \qquad (23)$$

These equations have solutions (for $x$ large) of the form

$$U(x) = Au_1(x) + Bu_2(x)$$

$$\Phi(x) = A\phi_1(x) + B\phi_2(x) \quad , \qquad (24)$$

where

$$\left.\begin{aligned} u_1(x) &= e^{-Kx} \\ u_2(x) &= 0 \\ \phi_1(x) &= \frac{e}{\varepsilon} e^{-Kx} \\ \phi_2(x) &= e^{-\beta x} \end{aligned}\right\} \quad \text{for } x \text{ large, positive}$$

and

$$K \equiv \left(\beta^2 - \frac{\varepsilon\rho\omega^2}{c\varepsilon + e^2}\right)^{1/2}$$

Equation (23(a)) clearly has only one solution, $u_1 = e^{-Kx}$ in Eq. (24), and the corresponding potential solution $\phi_1$ is related to $u_1$ by

substituting $\phi_1'' = K^2\phi_1$ in Eq. (23(b)). Substitution of $U'' = \beta^2 U$ into Eq. (23(a)) shows that a solution with exponential dependence $e^{-\beta x}$ has $U = 0$, and Eq. (23(b)) then gives the solution $\phi_2 = e^{-\beta x}$ in Eq. (24). From Eq. (24) we can construct

$$W(x) = Aw_1(x) + Bw_2(x)$$
$$\Theta(x) = A\theta_1(x) + B\theta_2(x) \quad , \tag{25}$$

where

$$w_1(x) = u_1'(x)$$
$$w_2(x) = u_2'(x)$$
$$\theta_1(x) = \phi_1'(x)$$
$$\theta_2(x) = \phi_2'(x)$$

In Eqs. (24) and (25) the constants A and B are unknown, but their ratio will be determined by the conditions in Eqs. (21) and (22) at $x = 0$. Since solutions to a set of linear equations can always be multiplied by an arbitrary constant, only this ratio B/A is significant. We note that the solutions $u_1(x)$ and $\phi_1(x)$ are independent of the solutions $u_2(x)$ and $\phi_2(x)$ in Eq. (24), and hence, we expect a general solution of the form

$$\boxed{\begin{aligned} U(x) &= AU_1(x) + BU_2(x) \\ \Phi(x) &= A\Phi_1(x) + B\Phi_2(x) \end{aligned}} \qquad \boxed{\begin{aligned} W(x) &= AW_1(x) + BW_2(x) \\ \Theta(x) &= A\Theta_1(x) + B\Theta_2(x) \end{aligned}} \tag{26}$$

for <u>all</u> $x > 0$ . (The solutions for $x < 0$ are trivially determined by noting the condition that $U(x)$ is to be even or odd.) We now choose a point $x = +a$ , far away from zero and take

$$U_1(a) = u_1(a)$$

$$\Phi_1(a) = \phi_1(a)$$

$$W_1(a) = w_1(a)$$

$$\Theta_1(a) = \theta_1(a)$$

defined in Eqs. (24) and (25), as our initial values. The next step is to numerically integrate Eqs. (20) in to $x = 0$ , and read out the values $U_1(0)$, $\Phi_1(0)$, $W_1(0)$, $\Theta_1(0)$ from the computer. We then repeat the procedure for the functions $U_2(x)$, $\Phi_2(x)$, $W_2(x)$, $\Theta_2(x)$ , using $u_2(a)$, $\phi_2(a)$, $w_2(a)$, $\theta_2(a)$ as the initial values, and reading off $U_2(0)$, $\Phi_2(0)$, $W_2(0)$, $\Theta_2(0)$ from the numerical integration to $x = 0$ .

We now use these results in conjunction with Eqs. (21) and (22) to find the constants $A$ and $B$ . For $U(x)$-even modes, Eqs. (21) require

$$W(0) = AW_1(0) + BW_2(0) = 0$$

$$\Phi(0) = A\Phi_1(0) + B\Phi_2(0) = 0 \qquad (27)$$

For nonzero constants $A$ and $B$ to exist and satisfy these equations, the determinant of coefficients must equal zero, i.e.,

$$W_1(0)\Phi_2(0) - W_2(0)\Phi_1(0) = 0 \qquad (28)$$

Similarly, for U(x)-odd modes, the necessary condition for a solution is

$$\Theta_1(0)U_2(0) - \Theta_2(0)U_1(0) = 0 \tag{29}$$

The left side of Eqs. (28) and (29) will be functions of $\beta^2$, since the integration which yields $U_1(0)$, $\Phi_1(0)$, $U_2(0)$, etc. depends on the value of $\beta^2$ chosen. Hence, we define the functions

$$\begin{aligned} F(\beta^2) &\equiv W_1(0)\Phi_2(0) - W_2(0)\Phi_1(0) \\ G(\beta^2) &\equiv \Theta_1(0)U_2(0) - \Theta_2(0)U_1(0) \end{aligned} \tag{30}$$

The values of $\beta^2$ which zero $F(\beta^2)$ and $G(\beta^2)$ will correspond to the allowed even and odd modes which exist as guided waves in the domain wall.

In general, $F(\beta^2)$ and $G(\beta^2)$ will have many zeroes. The largest $\beta^2$ which zeroes $F(\beta^2)$ will mark the lowest order U(x)-even mode allowed. The largest $\beta^2$ which zeroes $G(\beta^2)$ will mark the lowest order U(x)-odd mode. As $\beta^2$ decreases, the zeroes alternate back and forth between $F(\beta^2)$ and $G(\beta^2)$ until no more trapping is possible. The smallest $\beta^2$ which zeroes one of these functions will be the highest (and most weakly trapped) mode allowed. By this procedure, we obtain the wave numbers $\beta_o, \beta_1, \beta_2 \cdots$ for the various modes propagating in the domain wall. Once we know these "eigenvalues" we can go back and read out the values of U(x) and $\Phi(x)$ by numerical integration.

## 2.4 Examples

To model domain walls, we must be able to choose reasonable representations for c(x), e(x), and $\varepsilon(x)$, the stiffness, piezoelectric, and

permittivity profiles. It stands to reason that these functions should all depend on the poling profile $P(x)$ in some fundamental way. This dependence should become more apparent in our future work. For now, we assume that $c(x)$ and $\varepsilon(x)$ can be represented by Gaussian like profiles

$$\begin{aligned} c(x) &= c_{44}^{E}\left(1 - \delta e^{-\alpha x^2}\right) \\ \varepsilon(x) &= \varepsilon_{11}^{S}\left(1 - \delta e^{-\alpha x^2}\right) \end{aligned} \tag{31}$$

where we have chosen $\delta = 0.1$ as representative. These functions have a full-width, half-maximum given by

$$\ell = \left(\frac{4\ \ell n\ 2}{\alpha}\right)^{1/2} \tag{32}$$

We will refer to $\ell$ as the "width" of the domain wall. The function $e(x)$ is also a function with a width $\ell$, and is intended to be directly proportional to experimental measurements of the poling profile $P(x)$.[2] For simplicity, we have assumed that $\rho(x)$ is constant.

For our numerical analysis, we have chosen PZT-8. By defining dimensionless coordinates $X$ such that

$$X \equiv \frac{x}{\ell} \tag{33}$$

we see that all problems treated will have a domain wall "width" of $\Delta X = 1$. The frequency $\omega$ will be "absorbed" into the parameter $\lambda$:

$$\lambda = \frac{2\pi}{k} = \frac{2\pi}{\omega}\left(\frac{c_{44}^{E}}{\rho}\right)^{1/2}. \tag{34}$$

For each problem, we specify the ratio $\ell/\lambda$ . If this ratio is large, then we should expect strong trapping; if it is small, we should expect weak trapping. Finally, we need to specify the value

$$R \equiv \frac{c_{44}^{E} \epsilon_{11}^{S}}{e_{15}^{2}} \tag{35}$$

for PZT-8, $R = 2.3$ (this is a dimensionless value). Now, we can see from Eq. (34) that for a fixed $P$ , higher frequencies $\omega$ result in larger $\ell/\lambda$ and hence better trapping.

If we work at 20 MHz, then $\lambda \approx 100$ μm in PZT-8, and we see from the figures that we can get fairly good waveguiding all the way down to about $\ell = 50$ μm (Fig. 3). If we widen our domain wall to $\ell = 100$ μm (Fig. 4), we get stronger trapping in the $U(x)$-even mode. We also note that a weakly trapped $U(x)$-odd mode appears at this width (Fig. 5). Of course, as we increase $\ell$ , the pre-existing modes become much more strongly confined, and more higher order modes appear (Fig. 6). For $\ell = 200$ μm , we have a second even mode and a second odd mode appearing (totaling four modes in all). Of course, if we were given a fixed domain wall of width $\ell$ , we could reproduce these effects by doubling frequency (instead of doubling $\ell$ ) to get better trapping and higher modes.

The next question which we address is whether or not a mode exists in the limit as $\ell/\lambda$ goes to zero. Going back to Eqs. (30), we found that $G(\beta^2)$ has no zeroes for $\ell/\lambda \leq 1/2$ and $F(\beta^2)$ has only one zero. This means that only the lowest order $U(x)$-even mode exists as the domain wall width approaches zero. We found that this mode persisted all the way down to $\ell/\lambda = 0.001$ , at which point the numerical program accuracy began to

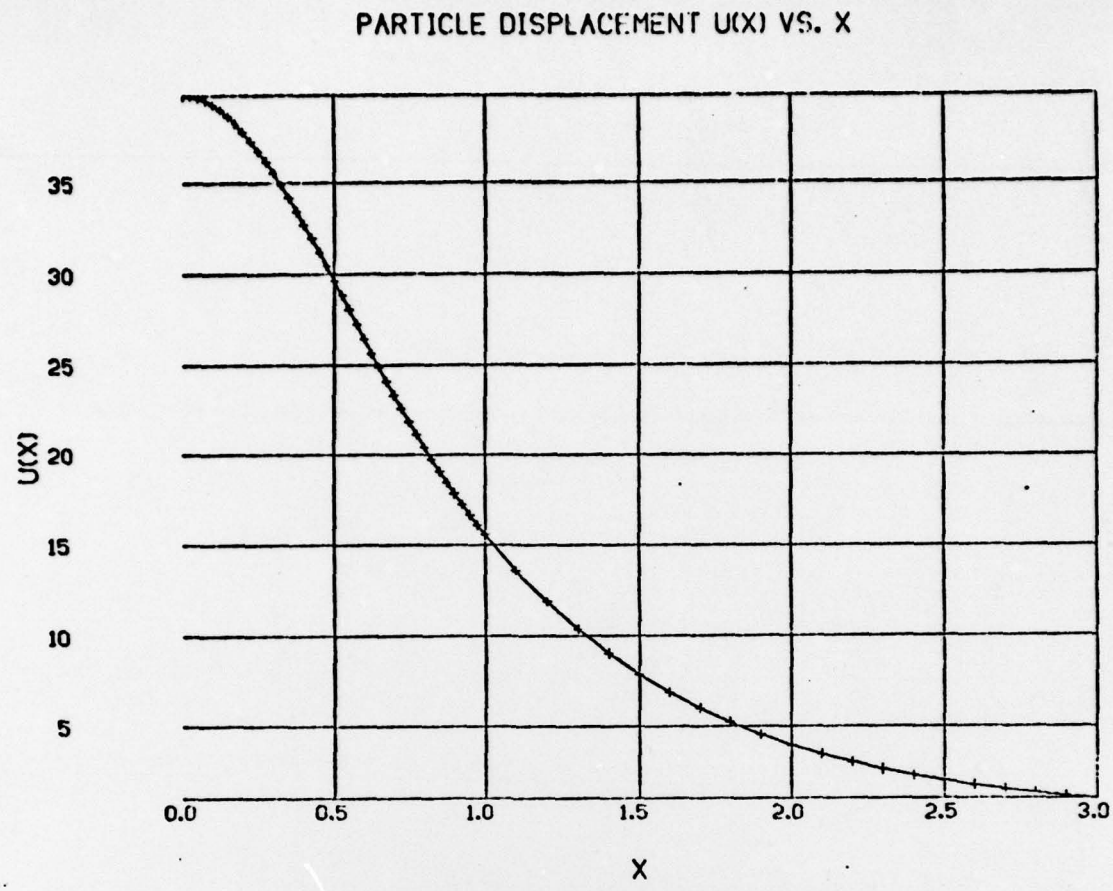


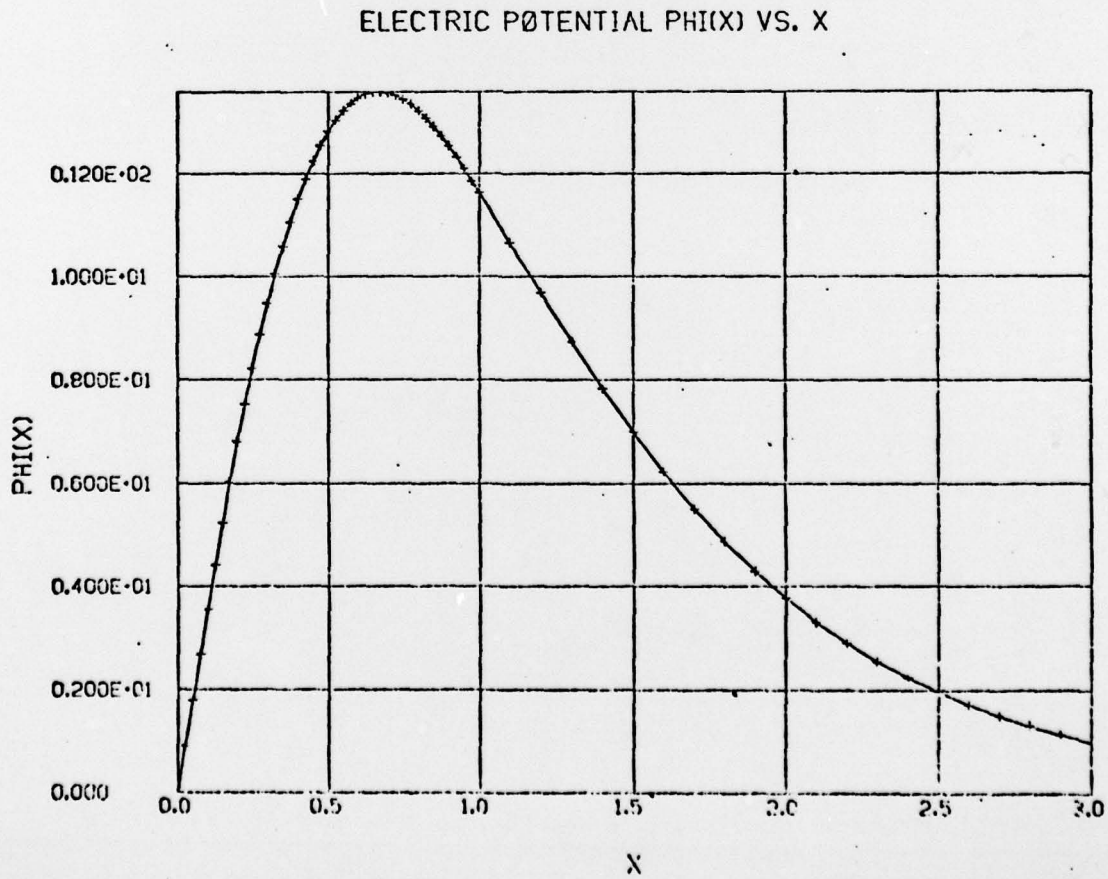


FIG. 3--Plot of $U(X)$ vs $\Phi(X)$ where the abscissa $X \equiv x/\ell$ is expressed in dimensionless units, and where the ordinate is scaled in relative units determined by the normalization $U(3.0) \equiv 1$, $\Phi(3.0) \equiv 1$, and $\ell/\lambda = 0.5$ .

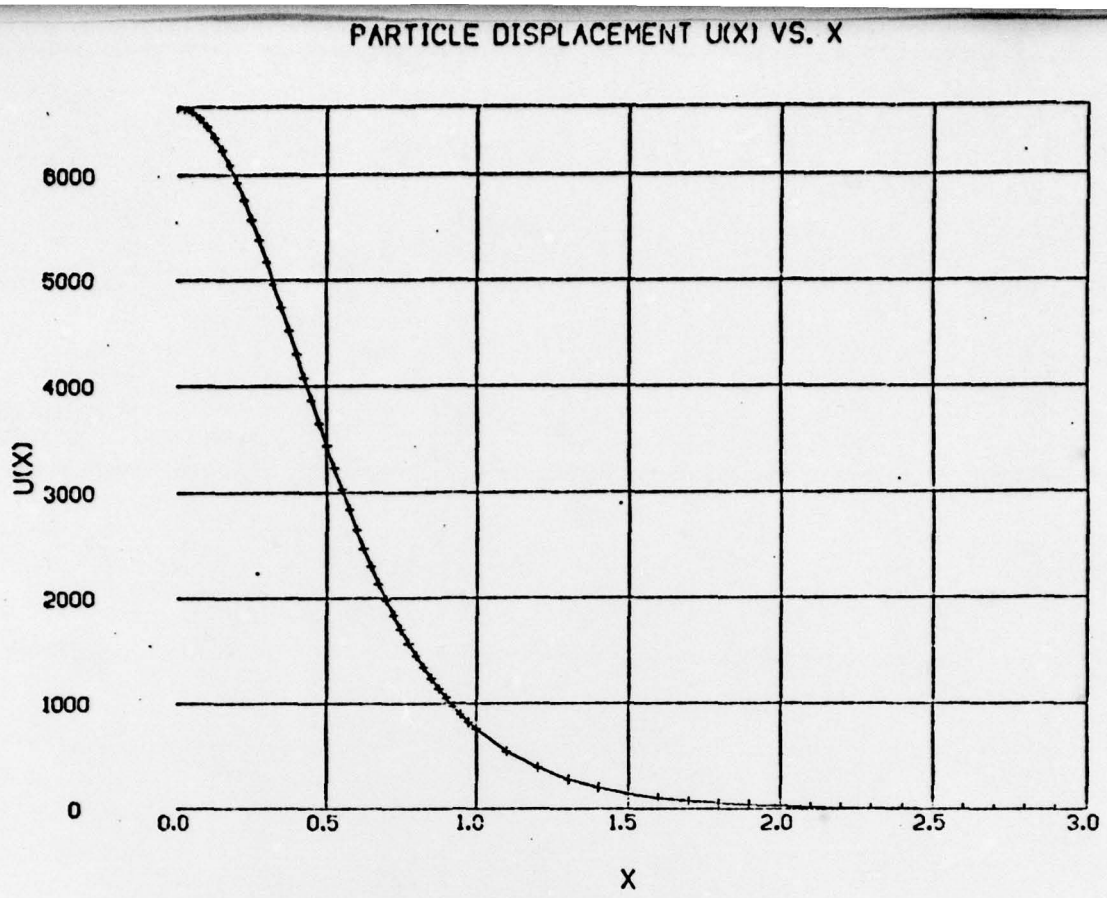


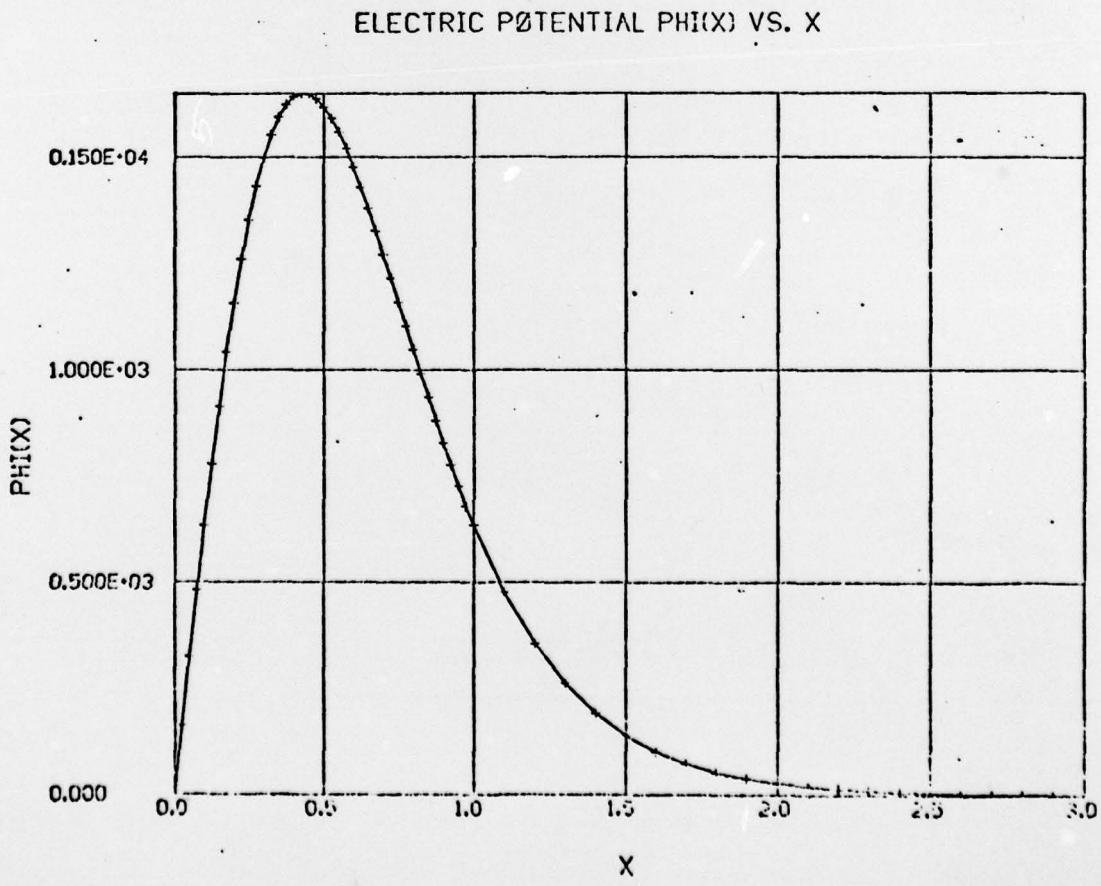


FIG. 4--The same as Fig. 3 except that $\ell/\lambda = 1$ .

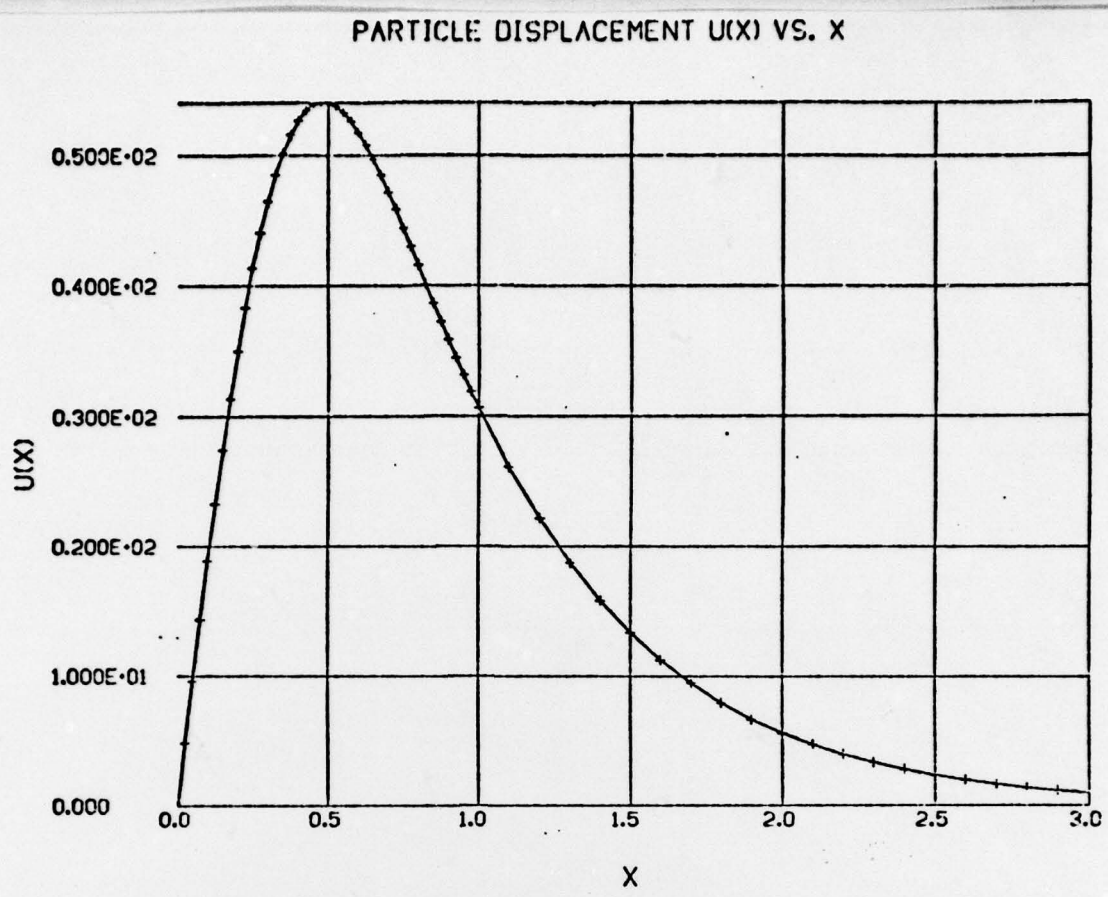


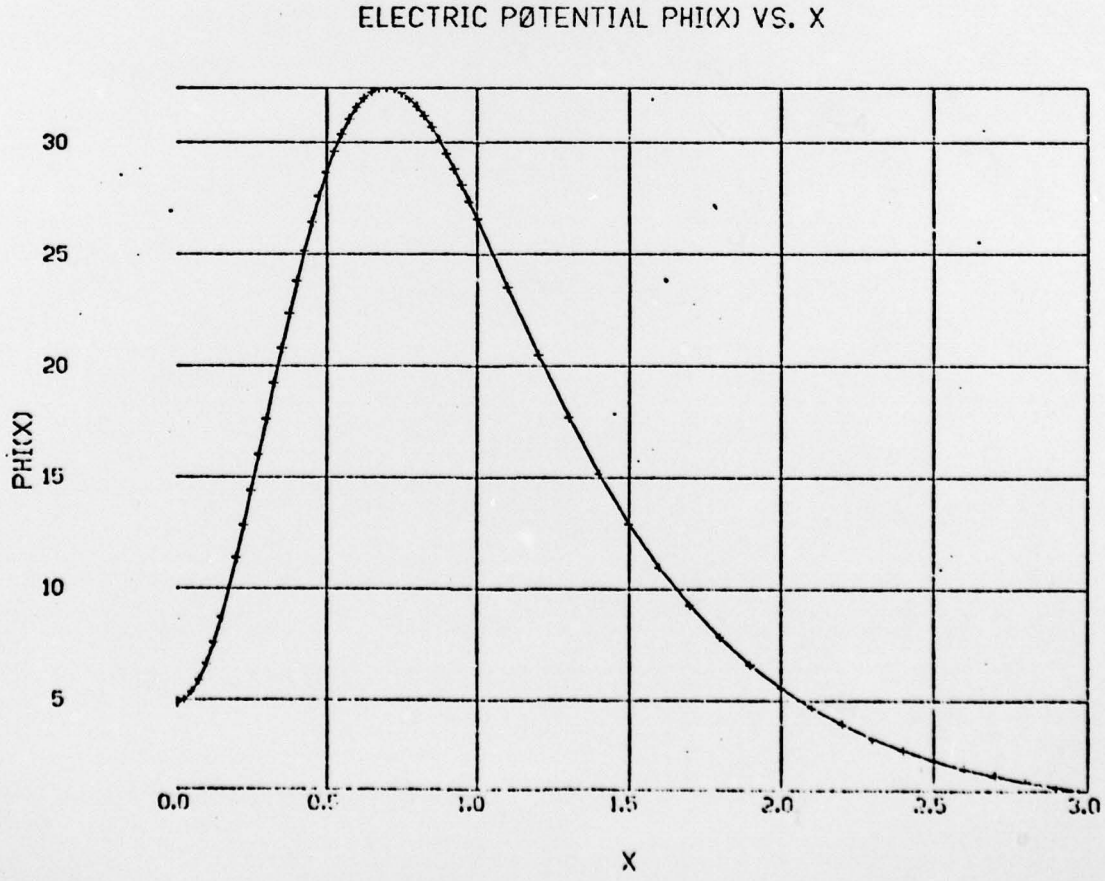


FIG. 5--Graphs showing the U(X)-odd mode, which appears at $\ell/\lambda = 1$ .

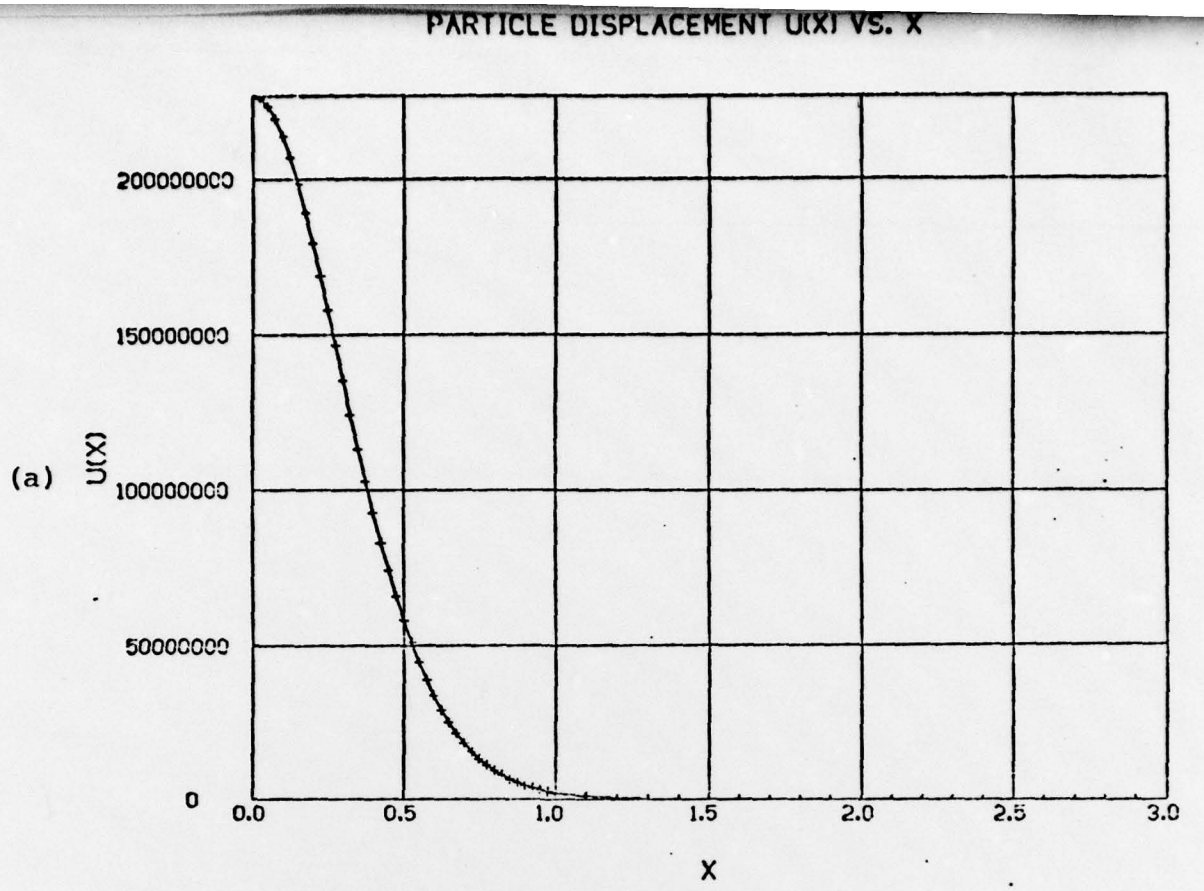


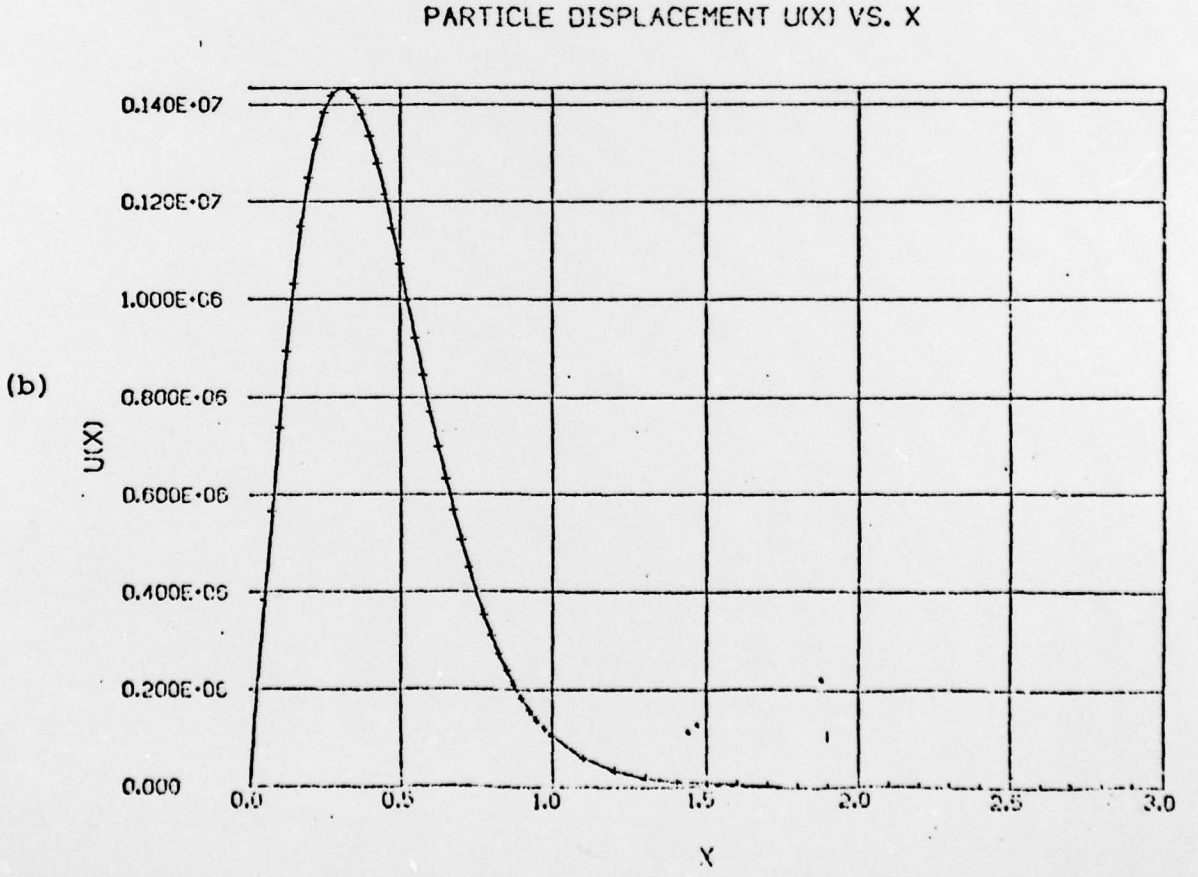


FIG. 6--Plots of U(X) for $\ell/\lambda = 2$ . Two even modes [(a),(c)] and two odd modes [(b),(d)] exist.

PARTICLE DISPLACEMENT U(X) VS. X
10000
5000
0
-5000
-10000
U(X)
0.0
0.5
1.0
1.5
2.0
2.5
3.0
X

(c)

PARTICLE DISPLACEMENT U(X) VS. X
60
40
20
0
-20
-40
-60
U(X)
0.0
0.5
1.0
1.5
2.0
2.5
3.0
X

(d)

FIGURE 6

limit the reliability of the result. At very small $\ell/\lambda$, the acoustic wave sees an essentially constant $c(x)$ and $\epsilon(x)$, and sees a piezoelectric function $e(x)$ which looks like a step function from $-e_{15}$ to $+e_{15}$. This limiting case problem has an analytical solution as demonstrated in the paper by Maerfeld-Tournois.[3] The solution is a surface interface wave which is evanescent in $x$ and propagating in $y$. The function $U(x)$ is even and $\Phi(x)$ is odd, which corresponds with the assumptions made about our lowest order $U(x)$ even mode. Furthermore, it can be shown that the wave number $\beta$ predicted by Maerfeld-Tournois is

$$\beta = \left(\frac{R + 1}{R + 2}\right)^{1/2} \cdot \frac{2\pi}{\lambda} \tag{36}$$

where $\lambda$ and $R$ are defined in (34) and (35) respectively. This result agrees with our theory as $\frac{\ell}{\lambda} \to 0$, as shown in Table I.

Table I

| $\ell/\lambda$ | Agreement with Maerfeld-Tournois |
|---|---|
| 0.20 | 4.1% |
| 0.10 | 0.89% |
| 0.06 | 0.12% |
| 0.04 | 0.08% |

This demonstrates excellent agreement in the narrow domain limit. Similarly, $U(x)$ and $\Phi(x)$ from our theory show excellent agreement with the form predicted by Maerfeld-Tournois as $\ell/\lambda$ becomes very small. We conclude that for $\ell/\lambda \leq 0.1$, we are safe in dispensing with our numerical

calculation, and using the simple analytic forms given by Maerfeld and Tournois:

$$U(x) = Ae^{-Kx}$$

$$\Phi(x) = A\frac{e}{\varepsilon}\left[e^{-Kx} - e^{-\beta x}\right] \tag{37}$$

for $x > 0$, where

$$K = \frac{2\pi}{\lambda} \cdot \frac{1}{[(R+1)(R+2)]^{1/2}} = \frac{\beta}{R+1}$$

and $\beta$ is given in Eq. (36).

## 2.5 Wave Scattering Problems

The procedure developed to compute guided wave modes in domain walls can be also applied to the problem of reflection and transmission of waves propagating through the domain wall (as opposed to along the domain wall). Of course, the waves propagating outside the domain wall will not be evanescent, so that new initial values (i.e. values at $x = \pm a$) must be chosen. Moreover $\beta^2$ will be determined by the equation

$$\beta = k \sin \theta_o$$

where $k$ is the wave number far outside of the domain wall region, and $\theta_o$ is the angle which the vector $\underline{k}$ makes with the x-axis. Therefore, $\beta$ will be smaller than before, and clearly fixed for each problem. To use our technique, we must restore $U(x)$ symmetry to the problem so that

we can use Eq. (21), or $U(x)$ antisymmetry to the problem so that we can use Eq. (22). This is done for symmetric $U(x)$ by launching a wave of amplitude $A$ from $x = -\infty$ and amplitude $A$ from $x = +\infty$.

If $R$ and $T$ are the reflection and transmission coefficient respectively, then, in the region $x > 0$, we will have an incoming wave of amplitude $A$, and an outgoing wave of amplitude $(R+T)A$. The sum $(R+T)$ is then chosen such that Eq. (21) is satisfied after integration of Eq. (20) into $x = 0$. For antisymmetric $U(x)$, we launch a wave of amplitude $-A$ from $x = -\infty$ and amplitude $+A$ from $x = +\infty$. The waves in $x > 0$ will now be an incoming wave of amplitude $A$, and an outgoing wave of amplitude $(R-T)A$. The difference $(R-T)$ is chosen such that Eq. (22) is satisfied. Hence, from $(R+T)$ and $(R-T)$ we can uniquely determine $R$ and $T$. By measuring $R$ and $T$ experimentally at different angles, we hope to be able to measure characteristics of the domain wall itself. This knowledge could enable us to better model the domain wall, and could be applied directly to our guided wave theory.

## 3. Conclusion

We have a numerical procedure for analysis of wave guidance or scattering at domain walls of practical interest, and are beginning to design some experiments. To this end we have made contact with the ceramics and materials group of Professor Eric Cross at Pennsylvania State University and have agreed to work co-operatively on the basis of their expertise in materials and ours in elasticity. Several areas we wish to explore together are:

1) Wave guidance experiments in the new strong electrostrictive ceramics, where an induced piezoelectric domain wall can be created by applying a dc electric field profile.

2) Wave guidance at boundaries in layered ceramics.

3) Possible studies of macroscopic models of grain boundaries.

We hope to begin with (1) immediately.

## 4. Presentations

"Interaction of Acoustic Waves with Ferroelectric and Ferroelastic Domain Walls," American Ceramic Society, Electronics Fall Meeting, Williamsburg, VA, September 16 - 19 -- to be prepared for publication.

"Acoustic Waves and Domain Walls," Pennsylvania State University, University Park, PA, November 8, 1979.

## 5. Visits

November 8 - Pennsylvania State University, University Park, PA.

## REFERENCES


1. B. A. Auld, Acoustic Fields and Waves in Solids, Vol. I (Wiley-Interscience, New York, 1973).

2. S. A. Farnow, "Acoustic Applications of the Zone Plate," Microwave Laboratory Report No. 2499, Stanford University, (December 1975), pp. 68-76.

3. C. Maerfeld and P. Tournois, "Pure Elastic Surface Wave Guided by the Interface of Two Semi-infinite Media," Appl. Phys. Lett. 19, 117-118 (1971).